NAVAL POSTGRADUATE SCHOOL
Monterey, California

THESIS

EFFECTS OF MUTUAL COUPLING IN SMALL DIPOLE ARRAY ANTENNAS

by

Yeo Chee Beng

March 2002

Thesis Advisor:	David Jenn
Second Reader:	Phillip Pace

THIS PAGE INTENTIONALLY LEFT BLANK

REPORT DOCUMENTATION PAGE			Form Approved OMB No. 0704-0188
Public reporting burden for this collection of information is estimated to average 1 hour per response, including the time for reviewing instruction, searching existing data sources, gathering and maintaining the data needed, and completing and reviewing the collection of information. Send comments regarding this burden estimate or any other aspect of this collection of information, including suggestions for reducing this burden, to Washington headquarters Services, Directorate for Information Operations and Reports, 1215 Jefferson Davis Highway, Suite 1204, Arlington, VA 22202-4302, and to the Office of Management and Budget, Paperwork Reduction Project (0704-0188) Washington DC 20503.			
1. AGENCY USE ONLY *(Leave blank)*	**2. REPORT DATE** March 2002	**3. REPORT TYPE AND DATES COVERED** Master's Thesis	
4. TITLE AND SUBTITLE: Title (Mix case letters) Effects of Mutual Coupling in Small Dipole Array Antennas			**5. FUNDING NUMBERS**
6. AUTHOR (S) Yeo Chee Beng			
7. PERFORMING ORGANIZATION NAME(S) AND ADDRESS(ES) Naval Postgraduate School Monterey, CA 93943-5000			**8. PERFORMING ORGANIZATION REPORT NUMBER**
9. SPONSORING /MONITORING AGENCY NAME(S) AND ADDRESS(ES) N/A			**10. SPONSORING/MONITORING AGENCY REPORT NUMBER**
11. SUPPLEMENTARY NOTES The views expressed in this thesis are those of the author and do not reflect the official policy or position of the Department of Defense or the U.S. Government.			
12a. DISTRIBUTION / AVAILABILITY STATEMENT Approved for public release, distribution is unlimited			**12b. DISTRIBUTION CODE**

13. ABSTRACT ***(maximum 200 words)***

In the classical approach of antenna theories, mutual coupling between elements is usually ignored. However, depending on the application, errors due to mutual coupling can be significant. This thesis investigates the effects of mutual coupling between elements in small dipole arrays via software simulations that use the Methods of Moment, a numerical technique that accounts for mutual coupling, as opposed to the classical approach, which does not. The simulations show that the active impedance of any element in an array depends on both the self and mutual impedances and that the terminal current phases, hence directivity, of an array are affected by mutual coupling such that the array pattern deviates from that defined by classical theoretical approach. In an active element pattern approach, the mutual couplings in an array are accounted for through the active element, making this approach a viable one to study the radiation patterns of practical dipole arrays. The examination of a small array provides a useful environment in which to develop, optimize and evaluate the radiating elements, thus providing better understanding of the effects of mutual coupling in antenna arrays and facilitating the design of corresponding compensation techniques in practical arrays.

14. SUBJECT TERMS Mutual coupling, mutual impedance, active element pattern, Patch			**15. NUMBER OF PAGES** 68
			16. PRICE CODE
17. SECURITY CLASSIFICATION OF REPORT Unclassified	**18. SECURITY CLASSIFICATION OF THIS PAGE** Unclassified	**19. SECURITY CLASSIFICATION OF ABSTRACT** Unclassified	**20. LIMITATION OF ABSTRACT** UL

NSN 7540-01-280-5500 Standard Form 298 (Rev. 2-89)
Prescribed by ANSI Std. 239-18

THIS PAGE INTENTIONALLY LEFT BLANK

Approved for public release, distribution is unlimited

EFFECTS OF MUTUAL COUPLING IN SMALL DIPOLE ARRAY ANTENNAS

Yeo Chee Beng
Major, The Singapore Army
B.Eng., King's College, University of London, England, 1991

Submitted in partial fulfillment of the
requirements for the degree of

MASTER OF SCIENCE IN SYSTEMS ENGINEERING

from the

NAVAL POSTGRADUATE SCHOOL
March 2002

Author: Yeo Chee Beng

Approved by: David Jenn
Thesis Advisor

Phillip Pace
Second Reader

Dan Boger
Chairman, Department of Information Sciences

THIS PAGE INTENTIONALLY LEFT BLANK

ABSTRACT

The phenomenon of mutual coupling in antenna arrays is a potential source of performance degradation, particularly in a highly congested environment such as the unmanned aerial vehicle where multitudes of arrays are accommodated in a constrained platform. This thesis investigates the effects of mutual coupling between elements in an antenna system via software simulations that use the Methods of Moments, a numerical technique that accounts for mutual coupling. The antenna configurations investigated comprise a single dipole and a three-dipole array, both above a simulated infinite perfect ground plane.

The simulation results show that the active impedance of any element in an array depends on both the self and mutual impedances and that the terminal current phases, hence directivity, of an array are affected by mutual coupling such that the array pattern deviates from that defined by classical theoretical approach which assumes identical element patterns. Results have been obtained for a single dipole and a three-dipole array above a simulated ground plane. The examination of a small array provides a useful environment in which to develop, optimize and evaluate the radiating elements, thus providing better understanding of the effects of mutual coupling and facilitating the design of corresponding compensation techniques in practical antenna arrays.

THIS PAGE INTENTIONALLY LEFT BLANK

TABLE OF CONTENTS

LIST OF FIGURES

THIS PAGE INTENTIONALLY LEFT BLANK

ACKNOWLEDGMENTS

I would like to express my most sincere gratitude to Dr David Jenn of the Naval Postgraduate School, Monterey, California for his guidance and invaluable contribution to the completion of this work.

I would also like to thank my wife Emeline for her support, without which I would not have been able to focus on my work.

THIS PAGE INTENTIONALLY LEFT BLANK

EXECUTIVE SUMMARY

In the classical approach of antenna theories, mutual coupling between elements is usually ignored. However, depending on the application, errors due to mutual coupling can be significant. The phenomenon of mutual coupling in antenna arrays is a potential source of performance degradation, particularly in a highly congested environment such as the unmanned aerial vehicle where multitudes of arrays are accommodated in a constrained platform.

This thesis investigates the effects of mutual coupling between elements in an antenna system via software simulations that use the Methods of Moments (MM), a numerical technique that accounts for mutual coupling, as opposed to the classical approach, which does not. The antenna configurations investigated comprise a single dipole and a three-dipole array, both above a simulated infinite perfect ground plane.

The frequency used in the simulations is 300 MHz. The basic dipole geometry consisted of a quadrilateral of length $L = 0.45\lambda$ and width $w = 0.005\lambda$. This length is chosen so that the current on the entire dipole is in phase, like in most practical applications. The length-to-width ratio is 90, which closely approximates an infinitely thin dipole.

The antenna analysis software packages, Patch and NEC-Win Professional, are used to determine the active impedance of a centrally voltage-excited dipole in free space and its mutual impedance with a perfect ground. Although Patch and NEC-Win Professional use the MM for antenna analysis, differences inherent in the coding and assumptions are expected. Slight variations were therefore made to the basic dipole geometry in NEC Win Professional. The dipole was placed parallel as well as perpendicular to the ground plane and its distance above the ground plane was varied. In the presence of an infinite ground plane, the driving point impedance of the dipole is found to be a function of terminal currents and mutual impedance. The mutual impedance is due to coupling between the dipole and the ground plane, and this effect diminishes as the dipole is moved away from the ground plane.

The effects of mutual coupling on the phase, directivity and active element patterns of a three-dipole array was investigated for dipole separations of 0.5λ and 0.375λ, with the array oriented horizontally with respect to the ground and placed at a height 0.25λ above it. In the transmit scenario, each dipole is centrally excited by a complex voltage of unit amplitude according to the dipole position in the array when the array is scanned. In the receive scenario, an incoming plane wave of unit amplitude is used. Mutual coupling changes the current magnitude, phase and distribution on the dipole, thereby 'distorting' the radiation vectors, giving rise to peaks and nulls in directions that are different from classical theoretical approximations.

The active element pattern depends on the position of the fed element in the array. The importance of the results on active element pattern comes from the fact that measurements of the active element patterns can give more directly the desired scan characteristics of an array under test and are therefore useful in predicting the scan performance of large phased arrays. Thus, active element patterns can be used to deduce the radiation properties of larger arrays.

The presence of mutual coupling variations in a finite antenna array causes amplitude and phase errors, the extent of which depends on the geometry and configuration of the array. Depending on the applications, such errors can be significant and result in severe system performance degradation, and must therefore be compensated for accordingly. In light of this, the research has also discussed further works with regard to compensating for the mutual coupling effects in dipole arrays. Even if these techniques do not result in the desired end-state of implementation in operational arrays, they can still be useful in simple laboratory or simulation set-ups to facilitate and enhance greater understanding of mutual coupling and its effects.

I. INTRODUCTION

A. BACKGROUND

Antenna arrays are widely employed in both commercial and military applications. Consequently, there is much research devoted to enhancing the performance of the various array configurations used. In particular, mutual coupling between the antenna elements in an antenna array is a potential source of performance degradation.

Depending on the application, errors due to mutual coupling can be significant. Mutual coupling variations between the elements are a source of amplitude and phase errors. The presence of mutual coupling distorts phase vectors of radiation sources [Ref. 1]. This can cause severe degradation of the tracking performance in radar as well as increasing the bit error rate in communication antennas, if it is not properly compensated. In effect, this phenomenon introduces a noise floor that precludes synthesis of high-quality patterns with very low side lobes or deterministic pattern nulls. Other possible effects appear in signal processing arrays, such as adaptive systems, which can be extremely sensitive to small errors due to the non-linear processing involved [Ref. 2].

For example, in the military, with the unmanned aerial vehicle (UAV) fast becoming a popular platform for a broad spectrum of battlefield applications, there is now an even greater impetus to better understand and counter the effects of mutual coupling. With an increasing payload to handle broader applications, it has become a major design challenge to accommodate the large number of electronic warfare and communications suites as well as the various other onboard processors on the UAV such that the individual components can function effectively on its own, as well as a collective whole. For this end-state to be possible, the mutual couplings that result from the interactions between the various components must be considered in the design process.

Mutual coupling is most significant between neighboring elements. It is often taken that the radiation pattern of an array of identical antenna elements is the product of an element factor and an array factor, on the assumption that all the elements have equal radiation patterns [Ref. 3]. For a practical array, this is not entirely true. For example, in a linear array consisting of a large numbers of elements, most of the embedded elements

experience approximately the same electromagnetic environment, thus exhibiting similar radiation characteristics. However, a few elements at both ends of the array encounter edge effects. This phenomenon becomes more pronounced in smaller arrays, where mutual coupling causes each element to see a different environment and consequently has a different radiation pattern from its neighboring elements.

The demand, hence versatility, required of small phased arrays due to the lower cost necessitates that the effects of mutual coupling be understood and that compensation techniques be developed in the applications of such arrays.

B. OBJECTIVE OF STUDY

The vast majority of previous research has dealt with mutual coupling in an infinite array environment [Ref. 4 - 6]. This thesis presents a fundamental quantitative analysis of mutual coupling associated with a single dipole and a three-element array in their respective simulated operational environments. The mutual coupling effects on the impedance of a radiating elemental dipole and on the radiation patterns of the dipole array for both transmitting and receiving modes will be investigated.

The examination of a small array provides a useful environment in which to develop, optimize and evaluate the radiating elements. In essence, this study provides a better understanding of the effects of mutual coupling and facilitates the design of corresponding compensation techniques in practical antenna arrays.

C. APPROACH

Commercially available software packages employing such techniques as the method of moments (MM) and the finite element method (FEM) are used to study the mutual coupling effects of the different dipole array geometries in simulated array and ground plane environments.

Both Patch and NEC-Win Professional are first used to investigate the mutual coupling effect of a single dipole that is centrally excited by a voltage. Both tools use the MM technique.

Next, the mutual coupling effect of a three-element array is studied using Patch. The antenna topology under investigation is a linear array of horizontally oriented dipoles, each of which is excited by a complex voltage according to the dipole position in the array. The scenarios for transmit and receive modes as well as with terminal loading are also investigated. For each of the geometries studied, the impedance and pattern results obtained from simulations are compared with the corresponding theoretical results.

D. OVERVIEW

Chapter II gives a theoretical analysis of the impedance characteristics of a single dipole as a radiating element in free space as well as within the confine of a perfect ground plane, and of a planar three-element array. This is followed by a discussion of the MM as a numerical analysis technique to predict the impedances between elements of an antenna array due to mutual coupling. The principle of pattern multiplication in antenna radiation and antenna directivity will also be covered.

Chapter III describes the simulations conducted using the software tools and presents the results. The dipole and array under test are subject to different operating environments such as geometry and various load conditions. The results from the different tools are compared and discussed in relation to mutual coupling and its effects.

Chapter IV discusses possible compensation techniques that can be explored to help reduce the effects of mutual coupling in small dipole arrays.

Finally, Chapter V summarizes the research and suggests further work with regard to compensating for the mutual coupling effects in small dipole arrays.

THIS PAGE INTENTIONALLY LEFT BLANK

II. THEORY

A. DIPOLES

The properties of any array depend on the characteristics of the individual radiating elements. The dipole in its various forms constitutes one of the most widely used radiating elements in arrays. This section begins with a discussion of a dipole in free space, followed by an analysis of its characteristics in the presence of a perfect electric conducting (PEC) ground plane to illustrate the effect of mutual coupling.

1. Single Dipole in Free Space

The fundamental building block of a practical dipole is the ideal Hertzian dipole. The ideal dipole is an infinitesimal element with a current of uniform magnitude and phase. Therefore, the radiation field from a longer practical length dipole is essentially the vector sum (integration) of the contributions from all ideal dipoles weighted by the current distribution.

The dipole field pattern in an array is called the element pattern, EP, which is exactly $\sin\theta$ for the Hertzian dipole. On a finite dipole, the current amplitude and phase are no longer constant. For a short dipole where its length $L << \lambda/2$, the current is in phase but its amplitude is approximately triangular. For a half-wave dipole, the current is still in phase and its amplitude can be approximated by a sinusoid. For these dipoles, the radiation will be strongest in the direction normal to the dipole and weakest along the axis of the dipole. As the dipole length increases, the radiation pattern sharpens, until at a length of $\lambda/2$, the half-power beam width narrows from 90° to 78°. However, for longer dipoles, the current on some sections will be out of phase with others, leading to partial or total cancellation in the far field [Ref. 3]

The infinitely thin $\lambda/2$ dipole in free space has a center-fed radiation resistance of $73.1\,\Omega$. At dipole length $L = \lambda/2$, the impedance is slightly inductive and the total radiation impedance is $73.1 + j42.5\ \Omega$. This inductive impedance drops rapidly to zero as the dipole is foreshortened. For $L = 0.485\lambda$, the dipole is resonant and the input

impedance is $71.8\ \Omega$. Below resonance, the reactive component of the dipole impedance is capacitive. In the range below $\lambda/2$, the dipole radiation resistance decreases monotonically with length and is almost independent of diameter, whereas the reactive component depends heavily on diameter. The thinner antennas are more capacitive for a given length [Ref. 1].

In practice, a dipole has a finite length-to-diameter ratio. Additionally, the environment also affects its impedance. Both the radiation pattern and impedance are influenced by the presence of nearby objects. The most commonly encountered object is the ground plane, which is intentionally introduced to increase the dipole's directivity.

2. Single Dipole Above a Perfect Ground Plane

The dipole impedance will change if the antenna environment is varied. As the impedance changes, the current on the dipole may become redistributed and thus alter the dipole's radiation pattern.

The presence of a ground plane affects the dipole's impedance. Consider a single dipole above an infinite ground plane that is also a perfect electric conductor. The image theory can be used to derive the relationships between the excitation voltage, impedance and current of the dipole. The image-method equivalent of a current-carrying dipole above a PEC ground is shown in Figure 1.

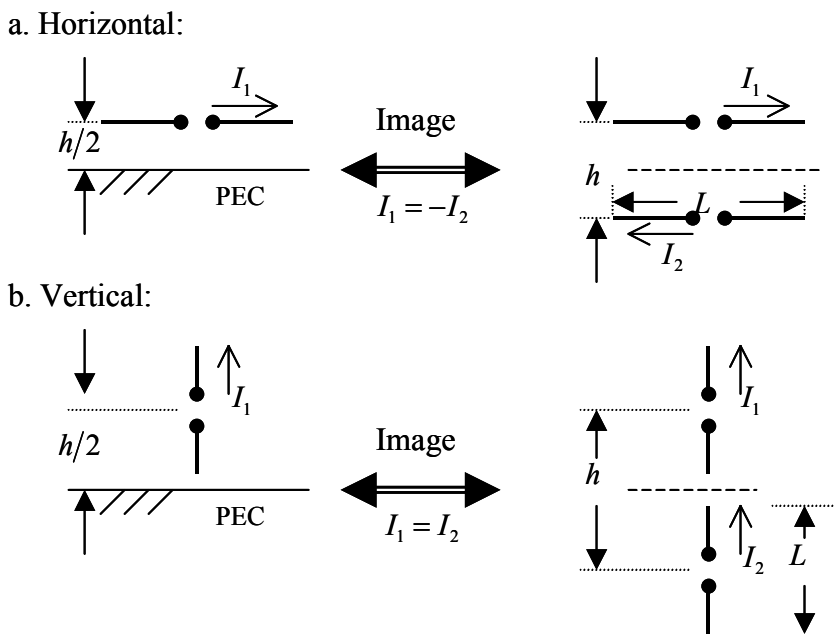

Figure 1. Image equivalent of a single dipole above ground.

In each case, the voltage across the dipole is governed by the following expression:

$$V_1 = I_1 Z_{11} + I_2 Z_{12} \tag{II.1}$$

where I_1 and I_2 are the source and image currents respectively, and Z_{11} and Z_{12} are the self and mutual impedances respectively.

Applying the image current relations to Equation (II.1), the voltage and active impedance across each dipole become as follows:

For the horizontal dipole,

$$V_1 = I_1 Z_{11} - I_1 Z_{12} \tag{II.2}$$

$$Z_1 = \frac{V_1}{I_1} = Z_{11} - Z_{12} \tag{II.3}$$

For the vertical dipole,

$$V_1 = I_1 Z_{11} + I_1 Z_{12} \tag{II.4}$$

$$Z_1 = \frac{V_1}{I_1} = Z_{11} + Z_{12} \tag{II.5}$$

Equations (II.3) and (II.5) give the impedance of a horizontal and vertical dipole over a ground plane respectively. In each case, the impedance is a function of the mutual impedance, Z_{12}, which is the result of mutual coupling between the dipole and the ground. By reciprocity, the mutual impedance of the image dipole is equal to that of the source dipole itself, i.e. $Z_{21} = Z_{12}$.

The image method in effect produces a pair of parallel dipole antennas, side-by-side in Figure 1a and collinear in Figure 1b respectively. Note that in order to apply the image method, the ground plane must be infinite. However, the method is often applied to finite ground plane if the edges extend sufficiently beyond the array of dipoles.

For the parallel side-by-side dipole antenna, the mutual resistance and mutual reactance are [Ref. 7]

$$R_{12} = 30\left\{2\cos(\beta h) - \cos\left[\beta\left(\sqrt{h^2 + L^2} + L\right)\right] - \cos\left[\beta\left(\sqrt{h^2 + L^2} + L\right)\right]\right\} \tag{II.6}$$

$$X_{12} = -30\left\{2\sin(\beta h) - \sin\left[\beta\left(\sqrt{h^2 + L^2} + L\right)\right] - \sin\left[\beta\left(\sqrt{h^2 + L^2} + L\right)\right]\right\} \tag{II.7}$$

where $\beta = 2\pi/\lambda$.

For the parallel collinear dipole antenna, the mutual resistance and mutual reactance are [Ref. 7]

$$\begin{aligned} R_{12} = {} & -15\cos(\beta h)\left[-2\cos(2\beta h) + \cos\left(2\beta(h - L)\right) + \cos\left(2\beta(h + L)\right) - \ln\left(\frac{h^2 - L^2}{h^2}\right)\right] \\ & +15\sin(\beta h)\left[2\sin(2\beta h) - \sin\left(2\beta(h - L)\right) - \sin\left(2\beta(h + L)\right)\right] \end{aligned} \tag{II.8}$$

$$\begin{aligned} X_{12} = {} & 15\sin(\beta h)\left[2\cos(2\beta h) - \cos\left(2\beta(h - L)\right) - \cos\left(2\beta(h + L)\right) - \ln\left(\frac{h^2 - L^2}{h^2}\right)\right] \\ & -15\cos(\beta h)\left[2\sin(2\beta h) - \sin\left(2\beta(h - L)\right) - \sin\left(2\beta(h + L)\right)\right] \end{aligned} \tag{II.9}$$

where in both cases,

$$Z_{12} = R_{12} + jX_{12} = Z_{21} = R_{21} + jX_{21} \tag{II.10}$$

In the presence of other dipoles, such as in a dipole array, mutual coupling will be more complex. Consequently, an array designer must consider the theoretical and empirical aspects of matching the dipole in an array environment.

B. DIPOLE ARRAYS

Dipole arrays are rarely designed to radiate into full space – the dipole elements are usually backed by reflectors, such as earth or wire grids. As the more central elements in an array are negligibly affected by the ground-plane edges, they can be viewed as being backed by an infinite ground plane. However, the few elements at both ends are significantly affected by mutual coupling, even if the ground plane is infinite.

To better understand this effect, consider a three-element dipole array parallel to and above an infinite ground plane. The image theory is again used to derive the relationships between the excitation voltage, impedance and current of the individual dipole. The image-method equivalent is shown in Figure 2.

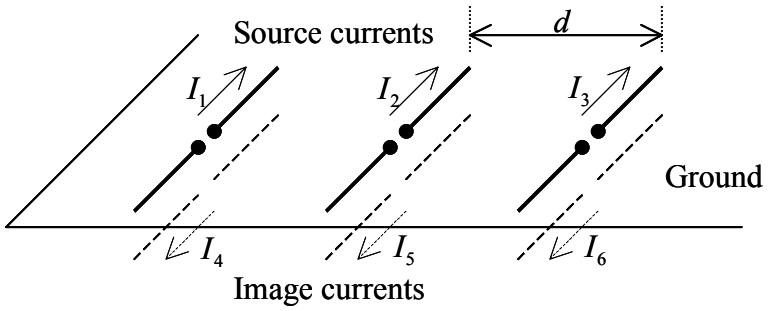

Figure 2. Image equivalent of a 3-dipole array above ground.

By the image method, in general,

$$I_4 = -I_1, \qquad I_5 = -I_2, \qquad I_6 = -I_3 \tag{II.11}$$

By symmetry, at broadside scanning,

$$I_1 = I_3, \qquad I_4 = I_6 = -I_1 \tag{II.12}$$

The currents in all the source dipoles as well as their image dipoles contribute to the voltage across each dipole element. For dipole 1, the voltage across it is given by the following expression:

$$\begin{aligned} V_1 &= I_1 Z_{11} + I_2 Z_{12} + I_3 Z_{13} + I4 Z_{14} + I_5 Z_{15} + I_6 Z_{16} \\ &= I_1 Z_{11} + I_2 Z_{12} + I_3 Z_{13} - I_1 Z_{14} - I_2 Z_{15} + I_6 Z_{16} \\ &= I_1 \left(Z_{11} - Z_{14} \right) + I_2 \left(Z_{12} - Z_{15} \right) + I_3 \left(Z_{13} - Z_{16} \right) \\ &= I_1 Z'_{11} + I_2 Z'_{12} + I_3 Z'_{13} \end{aligned} \tag{II.13}$$

where Z'_{1i} is the mutual impedance of dipole 1 with dipole i and its image.

By the same account, for dipoles 2 and 3,

$$V_2 = I_1 Z'_{21} + I_2 Z'_{22} + I_3 Z'_{23} \tag{II.14}$$

$$V_3 = I_1 Z'_{31} + I_2 Z'_{32} + I_3 Z'_{33} \tag{II.15}$$

The corresponding active impedances for the dipoles are derived as follows:

$$Z_1 = \frac{V_1}{I_1} = Z'_{11} + \frac{I_2}{I_1} Z'_{12} + \frac{I_3}{I_1} Z'_{13} \tag{II.16}$$

$$Z_2 = \frac{V_2}{I_2} = \frac{I_1}{I_2} Z'_{21} + Z'_{22} + \frac{I_3}{I_2} Z'_{23} \tag{II.17}$$

$$Z_3 = \frac{V_3}{I_3} = \frac{I_1}{I_3} Z'_{31} + \frac{I_2}{I_3} Z'_{32} + Z'_{33} \tag{II.18}$$

Equations (II.13) to (II.15) can be represented in matrix form as

$$[V] = [Z'][I] \tag{II.19}$$

For more complex geometries, such a simple analysis will not be possible. In place, numerical methods are used; most commonly, the Method of Moments (MM), and Finite Difference Method. The MM is the primary method used in the analysis and is discussed in the next section.

C. METHOD OF MOMENTS

The MM is a numerical technique that is applicable to arbitrary bodies. Essentially, it reduces the E-field integral equation (EFIE) into a matrix problem, the size of which is related directly to the electrical size of the antenna in terms of wavelength. Large bodies result in large matrices and, therefore, require large computers with fast processing units. The use of MM in the analysis and design of arrays of wire antennas (or scatterers) has significant advantages over the more classical methods used in treating arrays in that mutual coupling between array elements is taken completely into account. Furthermore, realistic assumptions can be made of the current distributions on the wires and the type of wire element array problem that can be considered is rather general, given that the array elements can be excited or loaded at any points. The use of MM to predict the impedances due to mutual coupling is discussed in the ensuing paragraphs [Ref. 8].

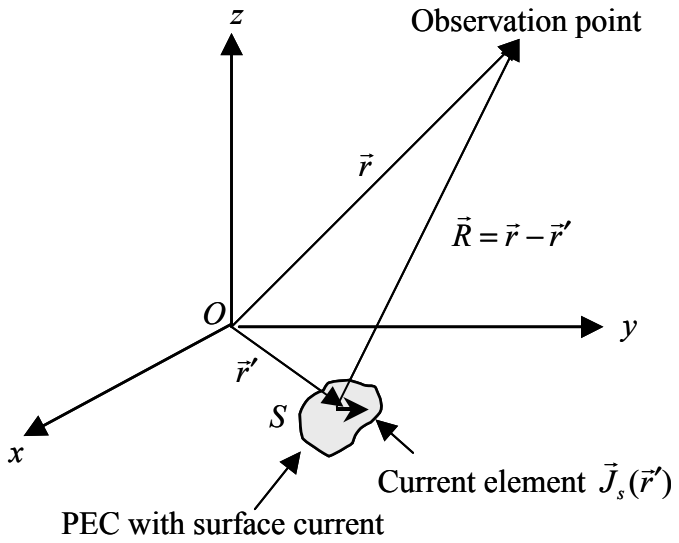

Figure 3. Derivation of EFIE. (After: [Ref. 8])

The first step in applying the MM is to represent the current on an arbitrary perfect electric conductor (PEC) by a series of unknown expansion coefficients I_n :

$$\overrightarrow{J_s}(\vec{r}) = \sum_{n=1}^{N} I_n \overrightarrow{J_n}(\vec{r}') \tag{II.20}$$

where $\overrightarrow{J_n}$ are the basis functions, and both I_n and $\overrightarrow{J_n}$ can be complex. The selection of the basis functions is an important consideration in the MM solution. Basis functions

should be mathematically convenient and be consistent with the behavior of the current. The series representation for the current density is then inserted into the EFIE.

The EFIE for a PEC is [Ref. 8]

$$\vec{E}_i(\vec{r})\big|_{\tan} = \sum_{n=1}^{N} I_n \iint_S \left\{ j\omega\mu \overrightarrow{J_n}(\vec{r}')G(\vec{r},\vec{r}') - \frac{j}{\omega\varepsilon}\left[\nabla' \cdot \overrightarrow{J_n}(\vec{r}')\right]\nabla' G(\vec{r},\vec{r}') \right\}_{\tan} ds' \tag{II.21}$$

where ω is the angular frequency (assuming a time dependence $e^{j\omega t}$), μ the permeability, ε the permittivity, $\vec{r}$ a position vector to an observation point on the surface of the PEC and $G(\vec{r},\vec{r}')$ the free space Green's function denoted by

$$G(\vec{r},\vec{r}') = \frac{e^{-j\beta R}}{4\pi R} \tag{II.22}$$

Next, define a set of weighting functions using Galerkin's method [Ref 8]. The weighting functions are chosen as follows:

$$\overrightarrow{W_m} = \overrightarrow{J_m^*} \tag{II.23}$$

where $m = 1, 2, \ldots N$.

Both sides of Equation (II.21) are multiplied by each of the weighting functions and integrated over its domain, deriving N equations of the form:

$$\iint_{Sm} \overrightarrow{W_m}(\vec{r}) \cdot \overrightarrow{E_i}(\vec{r})\big|_{\tan}\, ds = \iint_{Sm} \overrightarrow{W_m}(\vec{r}) \cdot \left\{ \sum_{n-1}^{N} I_n \times \iint_{Sn} j\omega\mu \overrightarrow{J_n}(\vec{r}')G(\vec{r},\vec{r}') - \frac{j}{\omega\varepsilon}\left[\nabla' \cdot \overrightarrow{J_n}(\vec{r}')\right]\nabla' G(\vec{r},\vec{r}') \right\}_{\tan} ds' \Big\} ds \tag{II.24}$$

Now, define the impedance element:

$$Z_{mn} = \iint_{Sm} ds \iint_{Sn} ds' \left[j\omega\mu \overrightarrow{W_m}(\vec{r}) \cdot \overrightarrow{J_n}(\vec{r}') - \frac{j}{\omega\varepsilon}(\nabla' \cdot \overrightarrow{J_n}(\vec{r}'))(\nabla \cdot \overrightarrow{W_m}(\vec{r}')) \right] G(\vec{r},\vec{r}') \tag{II.25}$$

where the surface divergence theorem has been applied:

$$\iint_S \overrightarrow{W_m} \cdot \nabla' G ds = \iint_S G(\nabla \cdot \overrightarrow{W_m}) ds \tag{II.26}$$

Let the right-hand side of Equation (II.24) be defined as

$$V_m = \iint_{Sm} \overrightarrow{W_m}(\vec{r}) \cdot \vec{E}_i(\vec{r}) ds \tag{II.27}$$

Equation (II.24) can now be written as

$$V_m = \sum_{n=1}^{N} I_n Z_{mn} \tag{II.28}$$

or in matrix form:

$$[V_m] = [Z_{mn}][I_n] \tag{II.29}$$

The matrix V_m is the excitation vector and Z_{mn} is the impedance matrix. The vector I_n contains the unknown expansion coefficients, which are determined by solving:

$$[I_n] = [Z_{mn}]^{-1}[V_m] \tag{II.30}$$

Once these expansion coefficients are determined, the series representation for the current, Equation (II.20), is defined and can therefore be used in the radiation integral to obtain the electric field at the observation point.

The MM is a powerful tool that provides rigorous solution for the induced current density on a body. Various proofs and theorems assure that the MM solution is rigorous under realistic conditions. In general, if the MM is properly applied, the series representation for the current will converge to the actual current as the number of basis functions is increased.

D. PATTERN MULTIPLICATON AND DIRECTIVITY

By the principle of pattern multiplication, the field pattern of an array consisting of similar elements is the product of the pattern of one of the elements (element pattern, EP) and the pattern of an array of isotropic point sources with the same locations, relative amplitudes, and phases as the original array (array factor, AF) [Ref. 3].

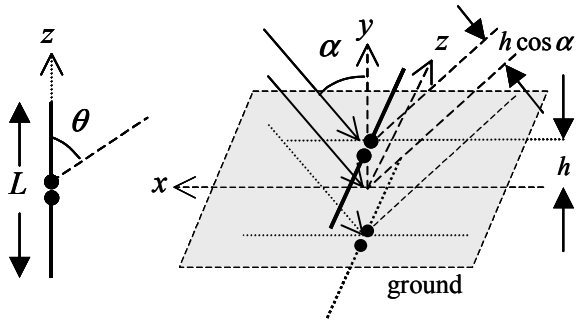

Figure 4. Single dipole parallel to and above perfect ground.

Consider a dipole of length L parallel to and of height h above a perfect ground plane, as shown in Figure 4. The normalized element pattern of the single dipole in free space is [Ref. 3]

$$EP = \frac{1}{L}\int_{L/2}^{L/2} e^{j\beta z'\cos\theta} dz' = \sin\theta \frac{\sin\left[(\beta L/2)\cos\theta\right]}{(\beta L/2)\cos\theta} \tag{II.31}$$

From Figure 4, the far field phase difference between the dipole and its image is $2j\sin(\beta h\cos\alpha)$, where α is the scan angle of an incoming (or outgoing) plane wave relative to the normal (y-axis) to the ground plane. The dipole and its image in effect form an array of two dipoles, with the array factor

$$\begin{aligned} AF &= 2j\sin(\beta h\cos\alpha) \\ &= 2j\sin(\beta h\sin\phi) \end{aligned} \tag{II.32}$$

where $\alpha = 90^\circ - \phi$, ϕ being the angle measured from the x-axis in the x-y plane.

By the principle of pattern multiplication, the overall field pattern F for the configuration in Figure 4 is therefore

$$F = EP \times AF = \sin\theta \frac{\sin\left[(\beta L/2)\cos\theta\right]}{(\beta L/2)\cos\theta} 2j\sin(\beta h\sin\phi) \tag{II.33}$$

Next, consider an equally spaced linear array of N identical dipoles, each dipole with a current of unit amplitude and uniform phase, at a height h above a perfect ground plane as shown in Figure 5. For this configuration, the element pattern consists of that for a dipole above the ground plane as defined by Equation (II.33), with the array factor

consisting of N isotropic point sources with the same locations, relative amplitudes, and phases as the original array.

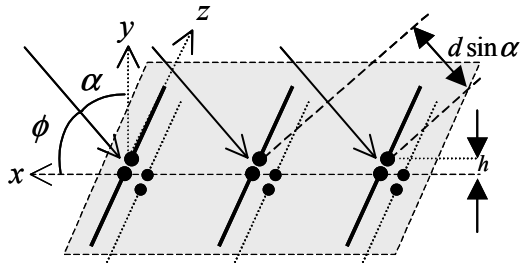

Figure 5. Equally spaced linear array of N identical dipoles above perfect ground.

From Figure 5, the phase difference between any two adjacent dipoles is

$$\psi = \beta d \sin\alpha = \beta d \cos\phi \tag{II.34}$$

The array factor is given by [Ref. 3]

$$AF = \sum_{n=0}^{N-1} e^{jn\psi} = e^{j(N-1)\psi/2} \frac{\sin\left(N\psi/2\right)}{\sin\left(\psi/2\right)} \tag{II.35}$$

When normalized, AF becomes

$$AF = \frac{\sin\left(N\psi/2\right)}{N\sin\left(\psi/2\right)} \tag{II.36}$$

Similarly, by the principle of pattern multiplication, the complete normalized field pattern F of the antenna array is then given by

$$F = \sin\theta \frac{\sin\left[\left(\beta L/2\right)\cos\theta\right]}{\left(\beta L/2\right)\cos\theta} 2j\sin(\beta h\sin\phi) \frac{\sin\left(N\psi/2\right)}{N\sin\left(\psi/2\right)} \tag{II.37}$$

Due to the ground plane, this field is radiated only over a half sphere above the ground plane. As a measure of the radiation intensity in a certain direction relative to an isotropic antenna, the directivity of this array can be derived. By definition, the directivity is given by

$$D\left(\theta,\phi\right) = \frac{4\pi}{\Omega_A} \tag{II.38}$$

where Ω_A is the beam solid angle defined by

$$\Omega_A(\theta,\phi) = \int_0^{\pi}\int_0^{\pi} |F|^2 \sin\theta d\theta d\phi \tag{II.39}$$

To summarize, in this section, the radiation pattern of an array of dipoles over an infinite ground plane is derived assuming identical element patterns. In practice, due to mutual coupling, the total array pattern, hence directivity, deviates from the ideal case. In addition, the mutual coupling effects depend on the frequency and scan direction. The simulations in the next chapter show the effects of mutual coupling.

III. SIMULATIONS AND RESULTS

A. SIMULATIONS

1. Simulation Parameters

The frequency used in the simulations is 300 MHz, which results in a one-meter wavelength. The basic dipole geometry consists of a quadrilateral of length $L = 0.45\lambda$ and width $w = 0.005\lambda$. This length is chosen so that the current on the entire dipole is in phase, like in most practical applications. The length-to-width ratio is 90, which closely approximates an infinitely thin dipole.

2. General Procedures

The antenna analysis software packages, Patch and NEC-Win Professional, are used to determine the active impedance of a centrally voltage-excited dipole in free space and its mutual impedance with a perfect ground. The dipole is placed parallel as well as perpendicular to the ground plane as in Figure 1 and its distance above the ground plane is varied. The results obtained are compared with those from Equations (II.6) to (II.9).

Next, the effect of mutual coupling on the phase and directivity of a dipole array over a perfect ground plane is investigated using Patch. The array topology comprises a linear array of three horizontally oriented dipoles, each of which is excited by a complex voltage according to the dipole position in the array, as shown in Figure 6. The scenarios for transmit and receive modes as well as with terminal loading are also investigated.

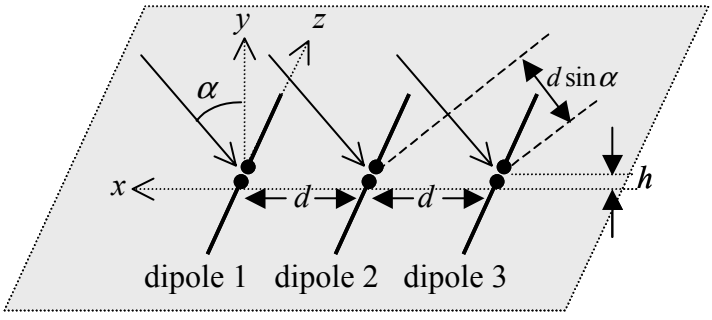

Figure 6. Three-dipole array above a ground plane.

3. Cylindrical Equivalence of a Quadrilateral

The quadrilateral dipole model is used in Patch. In NEC-Win Professional, a cylindrical dipole model is used instead. The equivalent cylindrical dipole has a length $L = 0.45\lambda$ and a radius $r = 0.00125\lambda$, where its radius is related to the width of the strip by $r = 0.25w$ [Ref. 9].

4. Convergence in Patch

Patch uses triangular sub-domains in the MM formulation. The patch geometry for the three-dipole array over a ground plane is depicted in Figure 7.

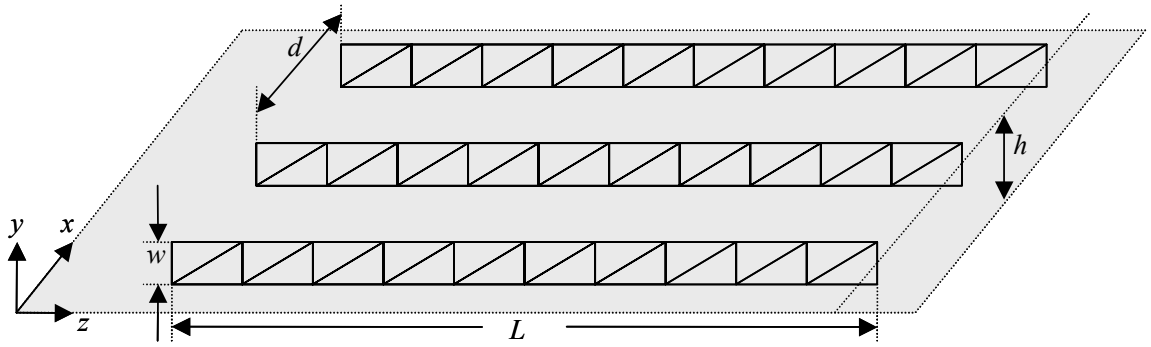

Figure 7. Representation of a three-dipole array in Patch.

For convergence, the segment length of each triangular patch should be less than 0.1λ. The smaller the segments, the more accurate the result will be. However, there will be a corresponding increase in computation time.

B. RESULTS

1. Impedance of a Dipole in Free Space

Using Patch, the current density at the center of the dipole is found to be $J = 1.7876 + j1.7136$ A/m, giving a total current $I = J \times w = 8.938 + j8.586$ mA. With a unit voltage excitation, the self-impedance of the dipole is calculated to be $Z_{11} = 58.3 - j55.89\ \Omega$.

Using NEC-Win Professional, the corresponding impedance obtained for eleven segments is $61.803 - j43.398\ \Omega$. Slight variations were then made to both the length and

radius of the cylindrical dipole. It was found that the closest agreement with Patch occurs when the cylinder length is shortened from 0.45λ to 0.44λ. At this length, the impedance becomes $58.24 - j58.89\ \Omega$. Although Patch and NEC-Win Professional use the same numerical technique for antenna analysis, differences inherent in the coding and assumptions are expected. This length of 0.44λ for the cylindrical dipole in NEC-Win Professional will be used in subsequent simulations.

As expected, the impedance obtained is capacitive, since the dipole length is less than 0.485λ, the approximate length at which resonance occurs. This result also agrees with the general behavior of input impedance based on actual measurements carried out by Brown and Woodward [Ref. 10].

2. Mutual Impedance of a Dipole Above Perfect Ground Plane

For each height above the ground plane, the impedance of the dipole Z_1 is obtained as in Section III.B.1. To derive the mutual impedance Z_{12}, its self-impedance Z_{11} is subtracted from its active impedance, Z_1, using Equation (II.5). The plots of Z_{12} against the height above the ground plane for a horizontal and vertical dipole are given in Figures 8 and 9 respectively.

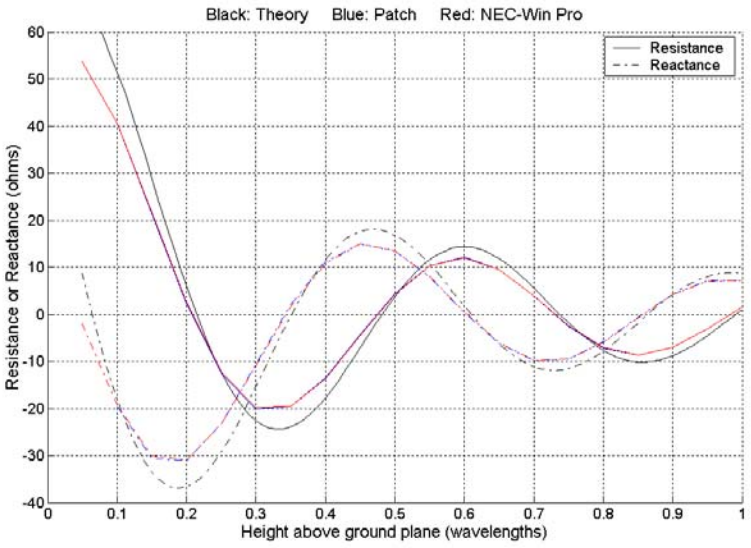

Figure 8. Mutual impedance of a horizontal dipole above ground plane.

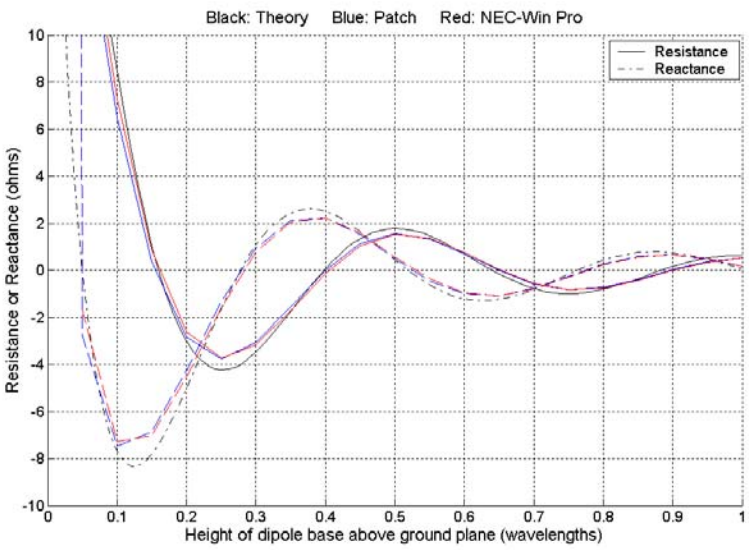

Figure 9. Mutual impedance of a vertical dipole above ground plane.

The mutual coupling between the dipole and the ground plane introduces Z_{12}. The plots in Figures 8 and 9 show that as the dipole is moved further away from the ground plane, both the resistive and reactive components of Z_{12} approach zero. This is expected because the coupling influence of the plane diminishes with increasing height, thus approximating a free space condition.

The mutual impedance obtained from Patch closely agrees with that from NEC-Win Professional. Both sets of simulation results are also in line with the corresponding theoretical values given by Equations (II.6) to (II.9). The results further establish the validity of MM as an analytical tool to determine the mutual coupling in an array. Since Patch and NEC-Win Pro give similar results, only Patch is used in subsequent analyses.

3. Effect of Mutual Coupling on 3-Dipole Array Above Perfect Ground Plane

The effect of mutual coupling on the phase, directivity and active element pattern of the 3-dipole array is investigated for dipole separation of 0.5λ and 0.375λ, with the array at a height 0.25λ above the infinite PEC ground plane. In the transmit scenario, each dipole is centrally excited by a complex voltage of unit amplitude according to the dipole position in the array when the array is scanned. In the receive scenario, an

incoming plane wave of unit amplitude is used. Thus, in the ideal situation, the phase should be linear and the amplitudes equal.

a. Phase

The effect of mutual coupling on the terminal phases of the array dipoles as a function of scan angle α is investigated for both transmit and receive modes.

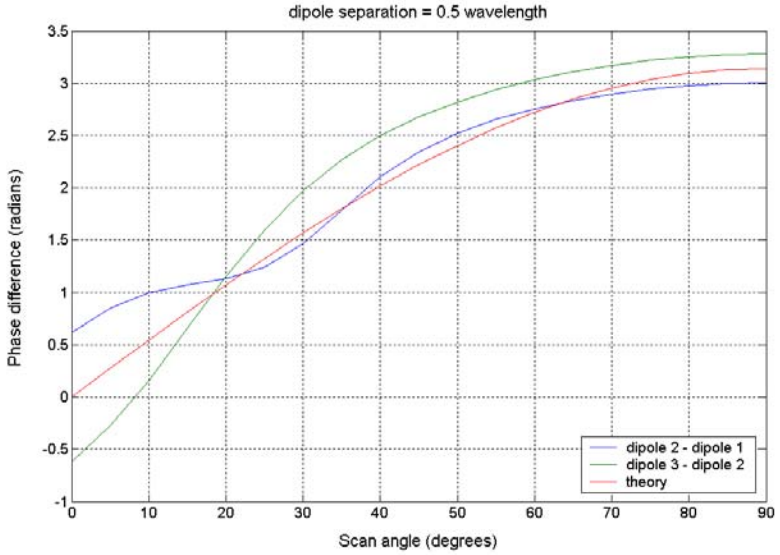

Figure 10. Phase difference on transmit as a function of scan angle α for $d = 0.5\lambda$.

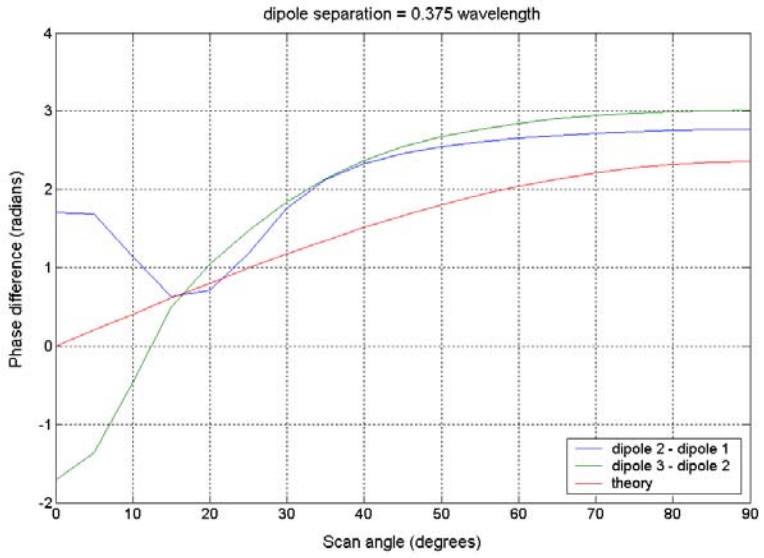

Figure 11. Phase difference on transmit as a function of scan angle α for $d = 0.375\lambda$.

In Figures 10 and 11, the blue curve is obtained by subtracting the terminal phase of dipole 1 from that of dipole 2 and the green curve is obtained by subtracting the terminal phase of dipole 2 from dipole 3. The red curve is the theoretical value for both the blue and green curves, as governed by Equation (II.34).

In theory, the terminal phase of dipole 3 leads that of dipole 2, which in turn leads that of dipole 1. This means that for scan angles other than broadside, both the blue and green curves should be greater than zero. The results in Figures 10 and 11 show that for small scan angles (less than 8° and 12° for the respective arrays), there is a phase lag for the green curve instead. At greater scan angles, the phases are also found to deviate from Equation (II.34). Both sets of results exhibit similar behavior.

The phase deviations between adjacent dipoles relative to the theoretical value are derived based on Figures 10 and 11 and plotted in Figures 12 and 13 respectively.

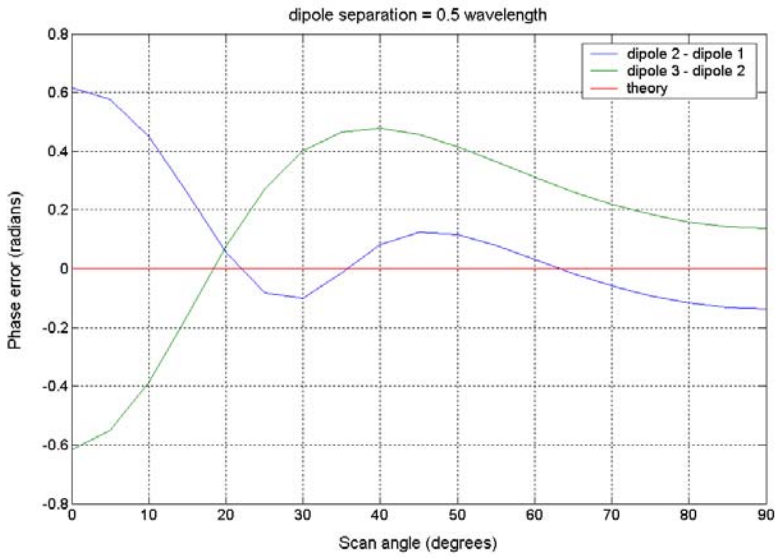

Figure 12. Phase deviation on transmit as a function of scan angle α for $d = 0.5\lambda$.

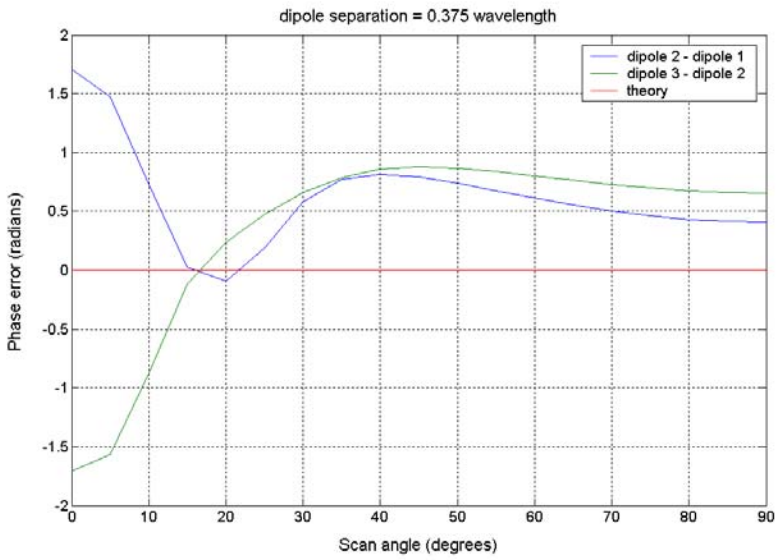

Figure 13. Phase deviation on transmit as a function of scan angle α for $d = 0.375\lambda$.

From Figures 12 and 13, it is observed that for both arrays, the phase deviations are greatest at broadside. For Figure 12, the deviation is minimum at scan angle of about 20° whereas for Figure 13, this occurs at about 16°. Beyond these angles, the deviations fluctuate but appear to smoothen out towards the array endfire.

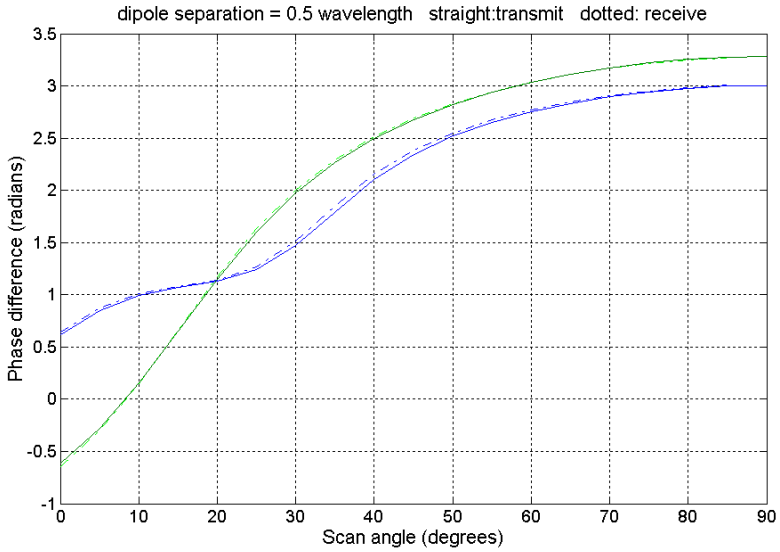

Figure 14. Comparison of phase difference between transmit and receive.

The phase difference between adjacent dipoles as a function of scan angle for $d = 0.5\lambda$ on receiving incoming plane waves is also investigated and compared with the corresponding values on transmit. The results are plotted in Figure 14. The two sets of results agree closely. This observation implies that the reciprocity theorem holds even in the presence of mutual coupling. The theorem therefore remains a very useful design tool.

As a result of mutual coupling, mutual impedances between the dipoles have been introduced upon excitation of the dipoles. This in turn distorts the phases at each dipole terminal, accounting for the deviations observed in Figures 10 to 13. Concomitantly, the directivity of the array is expected to vary with scan angle. The effect on directivity will be investigated in the next section.

b. Directivity

The effect of mutual coupling on array directivity in the transmit mode as a function of scan angle α is investigated.

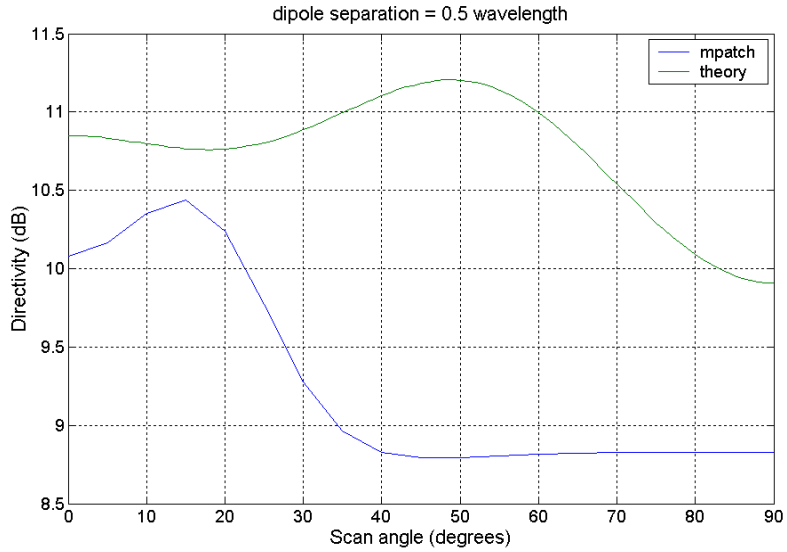

Figure 15. Array directivity on transmit for $d = 0.5\lambda$.

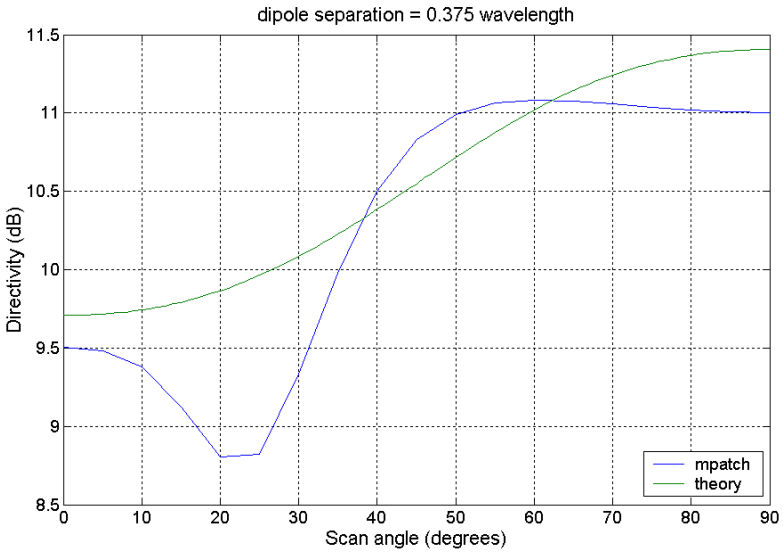

Figure 16. Array directivity on transmit for $d = 0.375\lambda$.

From Figure 15, for $d = 0.5\lambda$, the realized array directivity is less than the theoretical values obtained from Equations (II.38) and (II.39) at all scan angles. The difference is minimum at scan angle of 15° and maximum at scan angle of 50°. At broadside, the difference is about 0.7 dB. From Figure 16, for $d = 0.375\lambda$, for most scan angles, the realized directivity is also less than the theoretical values. For this array, the difference at broadside is about 0.25 dB

The assumption made in arriving at Equation (II.39) is that the element terminal currents are proportional to their excitations, the current distributions on the elements in the array are identical and pattern multiplication is valid. However, in a real array, the elements interact with each other and alter the currents, thus impedance, from that which would exist if the elements were isolated. This interaction, or mutual coupling, changes the magnitude, phase and distribution of current on each element and in turn is manifested in the loss of directivity of the arrays, hence the results obtained in Figures 15 and 16.

c. Active Element Pattern

The active element pattern of three-dipole array is obtained by centrally exciting a single element in the array with a unit voltage, with the other two elements terminated in loads of $50\,\Omega$. Three cases are investigated: (1) all the dipoles are centrally excited, (2) the center dipole, i.e. dipole 2, is centrally excited and (3) a side dipole, dipole 3, is centrally excited. The pattern plots for dipole separation of $d = 0.5\lambda$, $d = 0.375\lambda$, $d = 0.25\lambda$ are given in Figures 17 to 19 respectively.

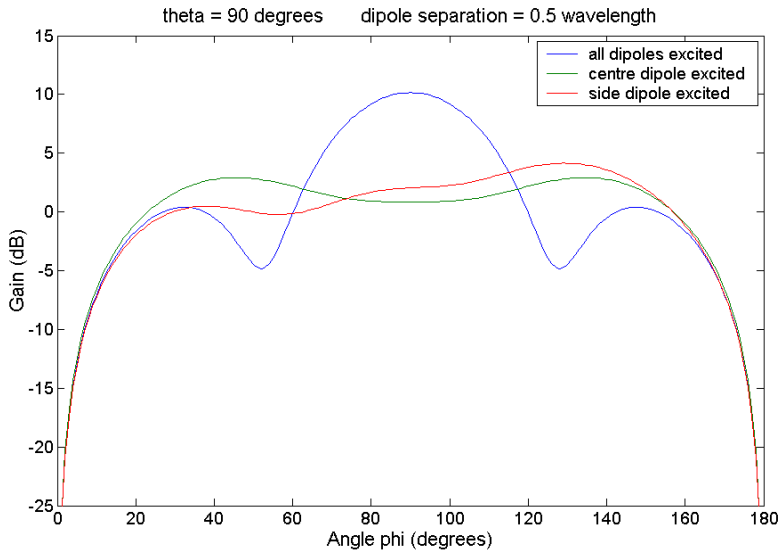

Figure 17. Active element patterns for $d = 0.5\lambda$.

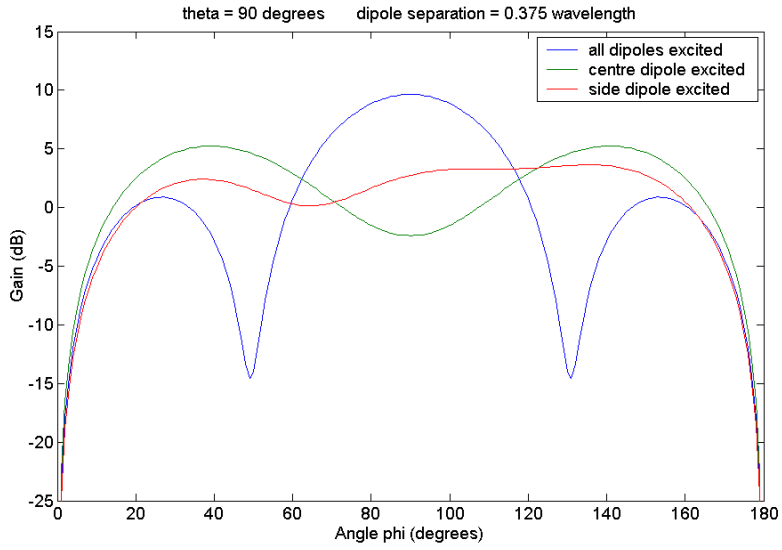

Figure 18. Active element patterns $d = 0.375\lambda$.

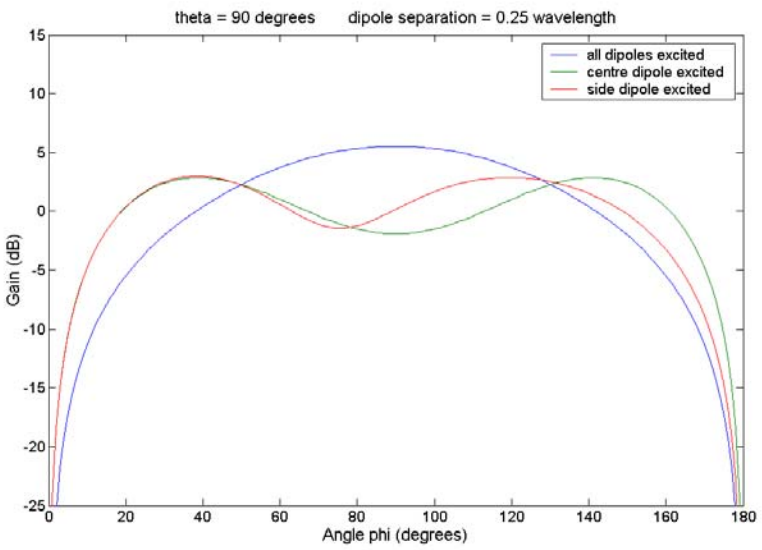

Figure 19. Active element patterns for $d = 0.25\lambda$.

In Figures 17 to 19, the red and green curves represent the active element patterns of the array as defined by Case (2) and Case (3) respectively. These patterns are different from what is expected of an isolated radiating dipole above a perfect ground, as defined by Equation (II.33). This is due to mutual coupling between the radiating dipole and its adjacent dipoles, which causes currents to be induced on the adjacent dipoles. Consequently, the adjacent dipoles also radiate power, albeit at a lower level compared to the power radiated from the excited dipole. In Case (2), because the excited dipole is centrally located, the induced currents, hence impedances, on dipole 1 and dipole 3 are equal (Equations (II.12), (II.16) and (II.18)). Consequently, the green curve is symmetrical about broadside, as opposed to the skewed effect observed in the red curve. In addition, the red curve shows gain reductions at scan angles of about 35°, 25° and 15° for $d = 0.5\lambda$, $d = 0.375\lambda$ and $d = 0.25\lambda$ respectively. At these corresponding scan angles, Figures 15 and 16 on directivity show comparable drops in gain when scanned to these angles. This observation agrees with the theoretical analysis made by Pozar [Ref. 12].

The blue curve represents the gain contributed by all the three radiating dipoles in the array and the corresponding mutual coupling effects. As a result, its gain at broadside is higher than those of the other two curves. In theory, at broadside, gain is

proportional to the array dimension, thus accounting for the observations made where the corresponding gain is highest for $d = 0.5\lambda$ and lowest for $d = 0.25\lambda$. However, side lobes exist for the arrays with $d = 0.5\lambda$ and $d = 0.375\lambda$. Ideally, nulls (zero gain) would exist between the main lobe and sidelobes, but mutual coupling causes a filling in of the nulls.

C. DISCUSSIONS OF RESULTS

The effect of mutual coupling diminishes as the separation between dipoles increases, i.e. it is most significant between neighboring elements, and this effect is more pronounced when the dipoles are placed side by side than when they are collinear. These observations are also intuitively true. In the former, a large separation approximates a free space condition, and in the latter, the effective surface area for interaction is much reduced for collinear dipoles as compared to side-by-side dipoles. The driving point impedance, or active impedance, is found to be a function of terminal currents and mutual impedance.

In a scanned array, the phases of the terminal currents are also varied under the influence of mutual coupling, and the errors are found to be greatest at broadside and appear to smoothen out at the array endfire. This effect of mutual coupling in an array is manifested by the far field pattern, or more specifically in the simulations, the directivity of the array. As opposed to the classical theoretical approximation obtained by considering each element in isolation, the actual realized directivity include variations in the excitation currents as well as the patterns of each element acting under the influence of all coupling effects. Mutual coupling changes the current magnitude, phase and distribution on the dipole, thereby 'distorting' the radiation vectors, giving rise to peaks and nulls in directions that are different from theoretical approximations.

The radiation properties of an array can be evaluated using the approach of active element pattern, which is obtained by exciting only an element while match-loading all other elements in the array. The obtained active element pattern is then due to the direct radiation from the excited element combined with the fields re-radiated from the other elements, which in turn receive their power through spatial coupling with the excited element. This coupling is a function of element characteristic and the array geometry.

The active element pattern depends on the position of the fed element in the array, so that the edge elements will have different active element patterns from those of the elements near the center of the array. If the array is large, however, most of the elements will see a uniform neighboring elements environment and the pattern can be approximated as equal for all elements in the array. To represent the possibility of gain variations, the active element levels are relative to a reference element located at the center of the array.

The importance of the results on active element pattern comes from the fact that measurements of the active element patterns can give more directly the desired scan characteristics of an array under test and are therefore useful in predicting the scan performance of large phased arrays, as illustrated by the close relation between nulls in the active element patterns and losses in directivity.

THIS PAGE INTENTIONALLY LEFT BLANK

IV. COMPENSATION TECHNIQUES

A. INTRODUCTION

Arrays are now widely used in electronic warfare and communications applications. Mutual coupling between elements can impact the array performance. The mutual coupling terms for elements near the edges of an array are significantly different from those for elements in the interior of a large array. This edge effect is particularly significant for small arrays.

The simulations have shown that the active impedance of each dipole element in an array varies as a function of the beam scan angle due to mutual coupling. In general, this results in a loss in array directivity, hence gain. The reduction in gain degrades the performance of the array, thereby limiting its usefulness. For example, for small direction finding arrays, mutual coupling leads to large phase errors that degrade the angle of arrival estimates, while for large arrays that have ultra-low sidelobe amplitude distributions, mutual coupling can affect the sidelobe levels, even though the majority of elements are away from edges.

Much research work has gone into the compensating techniques for various array configurations. Each technique has its own advantages and disadvantages. In the context of the simulations done in this work, some possible compensation techniques so that the array can be steered over a wide scan angle without significantly affecting its performance are suggested and discussed in the ensuing section.

B. COMPENSATION TECHNIQUES

1. Modification Within the Feed Line

The goal of this technique is to reduce the input impedance variation with scan angle. Theoretically, this can be accomplished by adding loads to the transmitters or receivers via series impedance or terminated circulators, as shown in Figure 20. The compensating impedance Z_{c_i} $(i = 1,2,3)$ adds to the corresponding impedance Z_i in Equations (II.16) to (II.18). Thus, variations in the impedances from element to element

can be corrected. However, the same Z_c must be used for all angles and therefore only an average correction can be introduced. The circulators do not correct for mutual coupling per se, but isolate the transmitter from reflections, which change as a function of angle due to mutual coupling, from the elements. For this technique, the concomitant effects such as the intrinsic loss due to the modification and variation of realized gain and bandwidth with scan angle should be investigated in tandem.

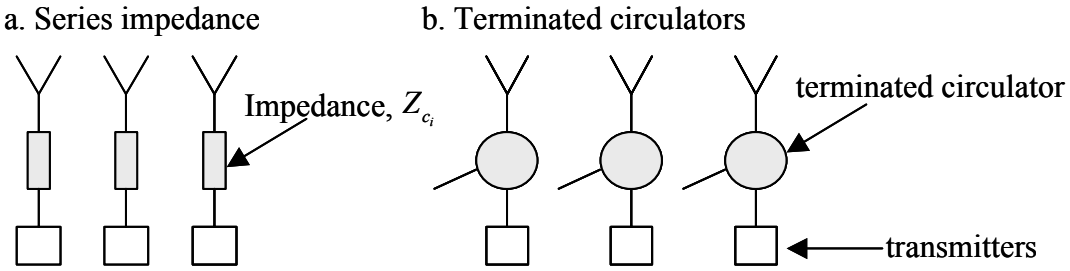

Figure 20. Techniques to impedance-match elements. (After: [Ref. 1])

2. Modification in External Environment of Array

This is based on the concept originally suggested and investigated by Edelberg and Oliner [Ref. 1]. One approach to mutual coupling mitigation is a simple add-on of dummy elements, which are loaded elements at the edges of the array, as shown in Figure 21. In a sense, the dummy elements "soften" the edge.

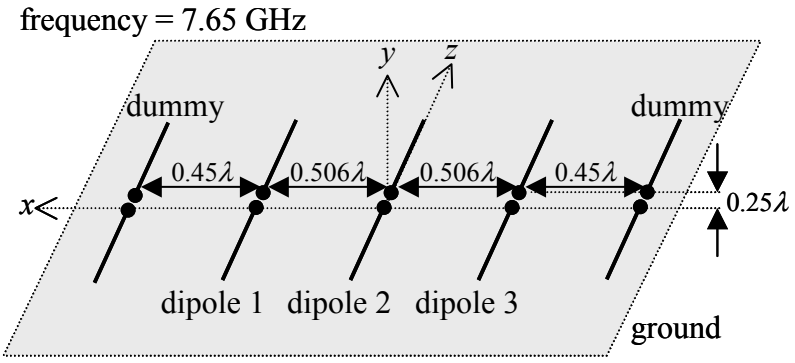

Figure 21. Three-dipole array with a dummy element on each side. (After: [Ref. 11])

Based on this configuration, preliminary results have been obtained using Patch and are given in Figures 22 and 23 [Ref. 11]. The data was generated by taking the

transmit active element patterns and using them as receive element patterns when all elements are combined on receive. Ideally, the phase across the array should be linear. The linear phase is subtracted out and the residual errors are plotted in the figures. Using dummy elements with a $50\,\Omega$ load, the maximum phase error has been reduced by about half. However, this load is not necessarily the optimum. For this technique, the number of dummies, their configurations and the optimum load conditions to closely approximate an infinite array environment need to be determined.

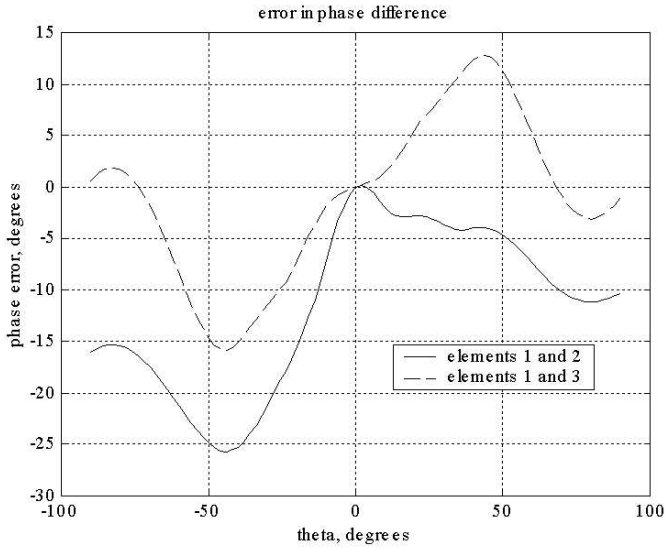

Figure 22. Phase error for the array without dummy elements. (From: [Ref. 11])

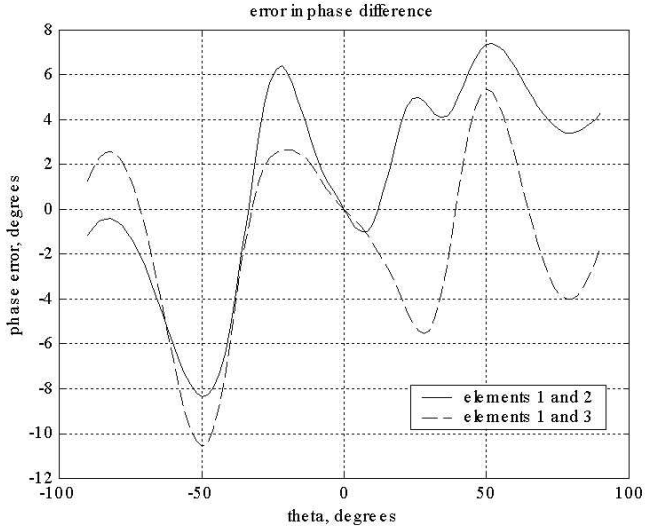

Figure 23. Reduced phase error for the array with dummy elements. (From: [Ref. 11])

3. Connecting Circuits

In this technique, matching circuits that vary with scan angle are used, so as to impedance-match phased arrays over wide scan angles. Such a conceptual network is shown in Figure 24 for collinear dipoles. Multi-port elements are used, with one of the feed points serving as a source for coupling corrections. A candidate element design that has shown promise for this application is a hybrid fed printed circuit dipole. It allows the adjustment of the free space coupling signals to be cancelled by the compensation network [Ref. 11]. The advantage of this approach is that it provides compensation that varies with angle. Hence, it has the potential to effectively correct for mutual coupling, which also varies with angle.

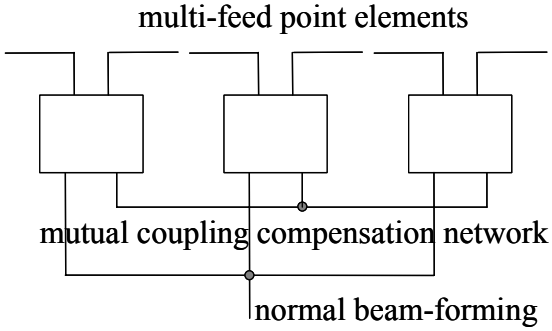

Figure 24. Compensation network integrated into a multi-feed array. (After: [Ref. 11])

The matching circuit must be connected in such a way as to preserve the symmetry of the array. In a planar array with identical elements, this simply means that the connecting circuits should be added in sets of parallel rows, each having identical circuits. Likewise, this technique attempts to achieve an infinite array environment. There are various forms that the connecting circuits may take. Capacitors, inductors, transmission lines or even more complex active networks can be employed, the choice being dependent on practical considerations, which vary from one antenna to another. To adopt this technique, the analysis, design and simulation of a mutual coupling compensation network and its integration with the beam-forming array need to be conducted.

With the requirements for operational arrays becoming more stringent and demanding, it is inevitable that for greater operational effectiveness, the development of compensation techniques to counter the effects of mutual coupling has also become an

integral design component. In practice, it is extremely difficult to completely control mutual coupling. Additionally, complexity and cost are also major design considerations.

THIS PAGE INTENTIONALLY LEFT BLANK

V. CONCLUSIONS

This thesis work has established the effects of mutual coupling between a radiating dipole element and its environment, and between radiating dipole elements within a 3-dipole array in a simulated operational environment. The simulations have shown that the active impedance of any element in an array depends on both the self and mutual impedances and that the terminal current phases, hence directivity, of an array are affected by mutual coupling such that the array pattern deviates from that defined by classical theoretical approach. In an active element pattern approach, the mutual couplings in an array are accounted for through the active element, making this approach a viable one to study the radiation patterns of practical dipole arrays. Although the results have only been obtained for a single dipole and 3-dipole array above a simulated ground plane, they are based on the use of MM, which accounts for mutual couplings and is generally applicable to any geometry. The results can therefore be extended to arrays of different geometries and configurations. The examination of a small array also provides a useful environment in which to develop, optimize and evaluate the radiating elements.

It should be noted that the presence of mutual coupling is not necessarily bad; in fact, Hannan has shown that mutual coupling is actually required in closely spaced infinite arrays to achieve idealized scanning performance [Ref. 13]. However, the presence of mutual coupling variations in a finite antenna array causes errors, the extent of which depends on the geometry and configuration of the array. Depending on the applications, such errors can be significant and result in severe system performance degradation, and must therefore be compensated for accordingly. In light of this, the research has also discussed further works with regard to compensating for the mutual coupling effects in dipole arrays. Even if these techniques do not result in the desired end-state of implementation in operational arrays, they can still be useful in simple laboratory or simulation set-ups to facilitate and enhance greater understanding of mutual coupling and its effects.

The next phase of this research should focus on the compensation techniques of dummy elements and compensation networks. Dummy elements are appealing because

they are simply an add-on solution that does not require redesign of an existing array. The optimum number, spacing and load conditions must be determined.

The compensation network depicted in Figure 24 would have to incorporate some complex weights (attenuators and phase shifters). The entire compensation network can be modeled using a combination of method of moments and scattering parameters as described in [Ref. 14]. This approach includes all the interactions between the elements, both via free space (i.e. mutual coupling) and through the feed network. It is conceivable that for a small array, a relatively compact solution for the compensation weights might be possible.

In conclusion, this study provides a fundamental understanding of the effects of mutual coupling in antenna arrays and facilitates the design of corresponding compensation techniques in practical arrays.

APPENDIX I. PATCH FILES

A. INPATCH FILE FOR CENTRALLY EXCITED ARRAY

A sample inpatch file for the centrally-excited three-dipole array at a scanning angle of 15° is as follows:

```
(Geometry)
  66  123
   1         0.000000E+00         2.475000E-01        -2.250000E-01
   2         0.000000E+00         2.525000E-01        -2.250000E-01
   3         0.000000E+00         2.475000E-01        -1.800000E-01
           .
           .
  65         0.500000E+00         2.475000E-01         2.250000E-01
  66         0.500000E+00         2.525000E-01         2.250000E-01
(Edges,faces,vertices)
   1    1    2
   2    1    3
   3    1    4
           .
           .
 122   64   66
 123   65   66
(Simulation parameters)
          1
          0         -1          0
          1
 v
          3
  21     14        .10000E+01    .00000E+00
  103    58        .68720E+00   -0.7264E+00
  62     36        .68720E+00    0.7264E+00
          0
          0
 .false.          0          0
          1
      90.000000       90.000000          1    0.000000E+00      180.000000
        181
          0
 .true.
          0
  3.000000E+08
    -1.000000
```

B. INPATCH FILE FOR PLANE WAVES INCIDENT ON ARRAY

A sample inpatch file for plane waves incident on the three-dipole array at different scan angle is as follows:

```
(Geometry)
  66  123
   1          0.000000E+00          2.475000E-01         -2.250000E-01
   2          0.000000E+00          2.525000E-01         -2.250000E-01
   3          0.000000E+00          2.475000E-01         -1.800000E-01
           .
           .
  65          0.500000E+00          2.475000E-01          2.250000E-01
  66          0.500000E+00          2.525000E-01          2.250000E-01
(Edges,faces,vertices)
   1    1    2
   2    1    3
   3    1    4
           .
           .
 122   64   66
 123   65   66
(Simulation parameters)
          1
          0          -1           0
          180
 p
          90         1          1 0 0 0
                     0          -1          0
 p
          90         2          1 0 0 0
 p
          90         178        1 0 0 0
                     0          -1          0
 .
 .
 p
          90         179        1 0 0 0
                     0          -1          0
 p
          90         180        1 0 0 0
                     0          -1          0
                        0
          0
  .false.           0          0
```

```
        1
   90       90    1    90    90
        1
                      0
.true.
3
 21
103
 62
  3.000000E+08
    -1.000000
```

THIS PAGE INTENTIONALLY LEFT BLANK

APPENDIX II. MATLAB PROGRAMS

A. IMPEDANCE OF DIPOLE OVER INFINITE PEC GROUND

The Matlab program to compute the impedance of a dipole in the presence of an infinite PEC ground is written based on Equations (II.6) to (II.9) in Chapter II. The program is as follows:

```
clear
clf

% geometry flag:
%  0 = horizontal, height = ht
%  1 = vertical, height = ht
flag=0;
if flag==0, disp('horizontal dipole over gp'),end
if flag==1, disp('vertical dipole over gp'),end
% total length L in wavelengths
L=0.45;
k=2*pi;
it=0;
efp=377/4/pi; eep=efp/2;

% horizontal dipole is side by side case with d=2*h
if flag==0
  for ht=0.05:.01:1
   it=it+1;
   H(it)=ht;
   d=2*ht;
   u0=k*d;
   u1=k*(sqrt(d^2+L^2)+L);
   u2=k*(sqrt(d^2+L^2)-L);
   R(it)=efp*(2*Ci(u0)-Ci(u1)-Ci(u2));
   X(it)=-efp*(2*Si(u0)-Si(u1)-Si(u2));
  end
end

% vertical is colinear case with spacing h=(L+s)and d=0)
if flag==1
  for ht=L/2+.01:.01:1.225
   it=it+1;
   H(it)=ht-L/2;    %height of dipole base above gp
   s=ht-L/2;
```

```
  h=L+2*s;
  v0=k*h;
  v1=2*k*(h+L);
  v2=2*k*(h-L);
  v3=(h^2-L^2)/h^2;
  R(it)=-eep*cos(v0)*(-2*Ci(2*v0)+Ci(v2)+Ci(v1)-log(v3))...
    +eep*sin(v0)*(2*Si(2*v0)-Si(v2)-Si(v1));
  X(it)=-eep*cos(v0)*(2*Si(2*v0)-Si(v2)-Si(v1))...
    +eep*sin(v0)*(2*Ci(2*v0)-Ci(v2)-Ci(v1)-log(v3));
  end
end

figure(1)
hold on
plot(H,R,'k-',H,X,'k-.'),grid
xlabel('Height above ground plane (wavelengths)')
ylabel('Resistance or Reactance (ohms)')
legend('Resistance','Reactance')
title(['Black: Theory     Blue: Patch     Red: NEC-Win Pro'])
```

B. ARRAY DIRECTIVITY

Equations (II.38) and (II.39) define the array directivity derived by classical approach. The Matlab program to plot the array directivity as a function of scan angle is as follows:

```
% This version: array of z-dipoles along x
clear
rad=pi/180;
ntl=3;      % number of dipole elements
h=0.25;     % height above ground plane at y=0
wdth=0.005; % strip width (not used)
dx=0.5;     % separation between dipole elements
x=[-1:1]*dx;
y=zeros(size(x));
freq=300e6;
wave=3e8/freq;
bk=2*pi/wave;

% dipoles are along the z axis
% y axis normal to aperture; infinite ground plane at y=0
%thetas=input('enter scan theta: ');
thetas=90
for count=1:91
```

```
   phis=count-1
us=sin(thetas*rad)*cos(phis*rad);
vs=sin(thetas*rad)*sin(phis*rad);
% read integration constants (gaussian quadrature)
     load gausq20.m
     xt=gausq20(:,1);
     at=gausq20(:,2);
     nt=length(xt);
% set the number of integration intervals (nt points per interval)
     ndivt=2;
     ndivp=8;
% integration interval in theta (degrees)
     S1=0*rad;
     S2=180*rad;
% integration interval in phi (degrees)
     Q1=0*rad;
     Q2=180*rad;
% generate integration points in theta and phi
     ds=(S2-S1)/ndivt;
     for i=1:ndivt+1
        SS(i)=(i-1)*ds;
        disp(['i,SS(i)= ',num2str(i),', ',num2str(SS(i))])
     end
     dq=(Q2-Q1)/ndivp;
     for i=1:ndivp+1
       QQ(i)=(i-1)*dq;
       disp(['i,QQ(i)= ',num2str(i),', ',num2str(QQ(i))])
     end
% subintervals in phi
     nphi=0;
     for ii=1:ndivp
     P1=dq/2;
     P2=(QQ(ii+1)+QQ(ii))/2;
      for n=1:nt
       nphi=nphi+1;
       wphi(nphi)=at(n);
       phi(nphi)=P1*xt(n)+P2;
      end
     end
% subintervals in theta
     ntheta=0;
     for ii=1:ndivt
     T1=ds/2;
     T2=(SS(ii+1)+SS(ii))/2;
      for i=1:nt
       ntheta=ntheta+1;
```

```
        wtheta(ntheta)=at(i);
        theta(ntheta)=T1*xt(i)+T2;
       end
      end
      ninteg=ntheta*nphi;
      disp(['number of int points= ',num2str(ninteg)])
% compute field at the integration points
      emax=0;
      sumx=0;
      phase=0;
      for iphi=1:nphi
        % disp(['phi=',num2str(phi(iphi)/rad)])
        for itheta=1:ntheta
         thr=theta(itheta);
         st=sin(thr); ct=cos(thr);
         phr=phi(iphi);
         cp=cos(phr); sp=sin(phr);
         sumAF=0;
% direction cosines in the global system
         u=st*cp; v=st*sp; w=ct;
% element factor sin(theta)
         EF=abs(st);
           for n=1:ntl
             argx=bk*x(n)*(u-us);
             argy=bk*y(n)*(v-vs);
             sumAF=sumAF+exp(j*(argx+argy));
           end
% have calculated the E-theta component
         Etheta=sumAF*EF*2*j*sin(bk*h*sin(phr));
         Ephi=0;
% all three of these give the same result (as expected)
         emagsq=abs(Etheta)^2;
         xint=emagsq*sin(theta(itheta));
       if emagsq>emax, emax=emagsq; thmax=thr/rad; phmax=phr/rad; end
       sumx=sumx+wphi(iphi)*wtheta(itheta)*xint;
       end   % end of theta loop
     end   % end of phi loop
     prad=T1*P1*sumx;
     gain=4*pi*emax/prad;
     gdb(count)=10*log10(gain);
  end
gdb;

scan=0:1:90;
gdb=fliplr(gdb)
plot(scan,gdb)
```

```
xlabel('Scan angle (degrees)')
ylabel('Directivity (dB)')
grid on
```

THIS PAGE INTENTIONALLY LEFT BLANK

LIST OF REFERENCES

1. Robert C. Hansen, *Microwave Scanning Antennas*, Vol. II, Array Theory and Practice, Peninsula Publishing, 1985.

2. Hans Steyskal and Jeffrey Y. Herd, "Mutual Coupling Compensation in Small Array Antennas," *IEEE Transactions on Antennas and Propagation*, Vol. 38, No. 12, December 1990.

3. Warren L. Stutzman and Gary A. Thiele, *Antenna Theory and Design*, Second edition, Wiley, 1998.

4. J. J. Lee, "Effects of Metal Fences on the Scan Performance of an Infinite Dipole Array," *IEEE Transactions on Antennas and Propagation*, Vol. 38, No. 5, May 1990.

5. S. Edelberg and A. A. Oliner, "Mutual Coupling Effects in Large Antenna Arrays I: Slot Arrays," *IEEE Transactions on Antennas and Propagation*, Vol AP-8, May 1960.

6. K. M. Lee and R. S. Chu, "Analysis of Mutual Coupling Between a Finite Phased Array of Dipoles and Its Feed Network," *IEEE Transactions on Antennas and Propagation*, Vol. 36, No. 12, December 1988.

7. John D. Draus, *Antennas*, McGraw Hill, 1950.

8. David C. Jenn, *Radar and Laser Cross Section Engineering*, AIAA, 1995.

9. E.A. Wolff, *Antenna Analysis*.

10. G. H. Brown and O. M. Woodward, Jr., "Experimentally Determined Impedance Characteristics of Cylindrical Antennas," *Proc. IRE*, Vol. 33, 1945.

11. David C. Jenn, notes on Array Coupling (unpublished), 2002.

12. D.M. Pozar, "The Active Element Pattern," *IEEE Transactions on Antennas and Propagation*, Vol. 42, No. 8, August 1994.

13. Peter W. Hannan, "The Element-Gain Paradox for a Phased Array Antenna," *IEEE Transactions on Antennas and Propagation*, Vol 36, No 12, July 1985.

14. D. Jenn, “A Complete Matrix Solution for Antenna Analysis,” *1989 IEEE AP-S Symposium Digest*, June 1989.

INITIAL DISTRIBUTION LIST

1. Defense Technical Information Center
   Ft. Belvoir, Virginia

2. Dudley Knox Library
   Naval Postgraduate School
   Monterey, California

3. Chairman
   Information Sciences Department
   Naval Postgraduate School
   Monterey, California

4. Professor David C. Jenn, Code EC/JN
   Department of Electrical and Computer Engineering
   Naval Postgraduate School
   Monterey, California

5. Professor Phillip E. Pace, Code EC/PC
   Department of Electrical and Computer Engineering
   Naval Postgraduate School
   Monterey, California

6. Dr. David G. Enders, Code 5700
   Naval Research Laboratory
   Washington, DC

7. Walter Elliott
   Southwest Research Institute
   San Antonio, Texas

8. Maj Yeo Chee Beng
   The Singapore Army
   Ministry of Defence
   Republic of Singapore